Biophysical Journal
Article

Biophysical Society

Sarcomere Stiffness during Stretching and Shortening of Rigor Skeletal Myofibrils

Nabil Shalabi,[1,2] Malin Persson,[2,3,4] Alf Månsson,[3] Srikar Vengallatore,[1] and Dilson E. Rassier[2,*]
[1]Department of Mechanical Engineering and [2]Department of Kinesiology and Physical Education, McGill University, Montreal, Québec, Canada; [3]Department of Chemistry and Biomedical Sciences, Linnaeus University, Kalmar, Sweden; and [4]Department of Physiology and Pharmacology, Karolinska Institutet, Stockholm, Sweden

ABSTRACT In this study, we measured the stiffness of skeletal muscle myofibrils in rigor. Using a custom-built atomic force microscope, myofibrils were first placed in a rigor state then stretched and shortened at different displacements (0.1–0.3 μm per sarcomere) and nominal speeds (0.4 and 0.8 μm/s). During stretching, the myofibril stiffness was independent of both displacement and speed (average of 987 nN/μm). During shortening, the myofibril stiffness was independent of displacement, but dependent on speed (1234 nN/μm at 0.4 μm/s; 1106 nN/μm at 0.8 μm/s). Furthermore, the myofibril stiffness during shortening was greater than that during stretching and the difference depended on speed (31% at 0.4 μm/s; 8% at 0.8 μm/s). The results suggest that the myofibrils exhibit nonlinear viscoelastic properties that may be derived from myofibril filaments, similar to what has been observed in muscle fibers.

INTRODUCTION

Actin and myosin have elastic properties that are central in chemo-mechanical energy transduction (1,2). They contribute to the stiffness of sarcomeres during stretching and shortening (3–5) and their elastic properties are used in the interpretation of a range of experimental studies in muscle biophysics (3,6,7). It is therefore interesting that optical tweezers studies with single myosin molecules showed evidence that myosin cross-bridges had nonlinear elasticity and a reduced stiffness when the cross-bridges were compressed to resist shortening (8). Although this effect is of great importance for understanding the molecular mechanisms of contraction, there is presently no conclusive evidence that the sarcomeres, containing all the myosin cross-bridges, also present nonlinear elasticity when organized in myofibril within the muscle cells.

Previous studies have investigated the stiffness and elastic properties of muscle fibers by removing ATP from the experimental solutions (6,9–14). Consequently, actin and myosin lock together in a rigor state where all the cross-bridges bind with the highest possible affinity (15). The use of such rigor preparations offers an interesting approach to evaluate the degree of nonlinearity of the cross-bridges by stretch-release experiments that are conceptually similar to the experiments with isolated proteins performed by Kaya and Higuchi in 2010 (5). If there is a delay between an initial stretch of a rigor fiber and a subsequent release, the cross-bridges that detach as a result of the stretch would have time to reattach to a neighboring actin site at a lower strain (16). Once released, those cross-bridges experience a negative strain and if they have a nonlinear stiffness, with a low stiffness for negative strain, the stiffness would be lower during the release than during the preceding stretch.

However, previous studies using rigor fibers had conflicting results; whereas some studies associated the sarcomere stiffness with the H-zone and the I-band, others associated the sarcomere stiffness with actin and myosin cross-bridges (6,10–12). The discrepancy in results is large—some studies showed an order-of-magnitude difference in stiffness (6,10–12). The disparity between studies is likely due to varying preparation and experimental procedures, as single fibers are affected by the action of cytoskeletal scaffolding proteins that affect sarcomere stiffness measurements (for a review, see (17)).

In recent years, studies with myofibril preparations added key insights about the mechanisms of muscle contraction and demonstrated several potential advantages in evaluating the elastic properties of sarcomeres (17). Myofibrils are the smallest organized units within the muscle hierarchical structure and are not influenced by the cytoskeletal scaffolding proteins present in fibers. They also represent a link between studies with single molecules and single fibers,

Submitted March 20, 2017, and accepted for publication October 5, 2017.
*Correspondence: dilson.rassier@mcgill.ca
Editor: David Thomas.
https://doi.org/10.1016/j.bpj.2017.10.007

filling an important gap in our understanding of muscle mechanics at the subcellular level. Until now, myofibrils have not been used for detailed evaluation of the sarcomere elasticity.

Here, we used psoas myofibrils in rigor and a custom-built atomic force microscope (custom-AFM) to stretch and shorten myofibrils using different amplitudes and speeds. We hypothesized that the stiffness of myofibrils reflects the same pattern observed in single molecule studies, but that they are more compliant than entire muscle fibers due to the lack of cytoskeleton proteins that connect myofibrils together inside the fibers.

METHODS

Ethical approval

The Animal Care Committee at McGill University and the Canadian Council on Animal Care approved the protocol to euthanize rabbits. Female New Zealand White Rabbits were obtained by Charles River Canada and were euthanized at an age between 4 months and a year. They were fed ad libitum and weighed between 2.5 and 3.5 kg. Exsanguination under general anesthesia was used to euthanize the rabbits. Accordingly, a subcutaneous injection was administered (premedication in 0.1 mg/kg Glycopyrrolate, 0.5 mg/kg Butorphanol, and 0.75 mg/kg Acepromazine) followed by an intramuscular injection (anesthetics in 35 mg/kg Ketamine, 5 mg/kg Xylazine).

Preparation of the myofibrils

Rabbits were euthanized and muscle fiber bundles were obtained from the major psoas muscle. The pieces were prepared and isolated based on previously documented procedures and solutions (3,18–21). The muscle fiber strips were excised (2–3 cm long) and then placed at 0°C for 4 h with rigor solution (100.6 mM KCl, 2.0 mM $MgCl_2.6H_2O$, 1.1 mM EGTA, 50.0 mM Tris; pH 7) mixed with protease inhibitors to avoid protein degradation (Protease Inhibitor Cocktail Tablets; Roche Diagnostics, Indianapolis, IN). The solution was then refreshed and an equal amount of glycerol was added for 15 h at 0°C. Afterwards, the entire solution was refreshed again and stored for at least 1 week at −20°C.

On the day of the experiments, a muscle fiber bundle was first equilibrated in rigor solution at 4°C for at least an hour. Then, 2–3 mm pieces were excised and isolated myofibrils were obtained after homogenizing three times at 12,000 rpm for 5 s, and three times at 28,000 rpm for 3 s (Power AHS250 Homogenizer with a 5-mm generator; VWR, Radnor, PA).

Instrumentation

The myofibrils were tested with a custom-AFM as previously described (17,22,23). Briefly, isolated myofibrils were placed into rigor solution inside a thermally controlled chamber that was maintained at 10°C. An inverted microscope with phase-contrast illumination was used to recognize the striation pattern on the myofibrils, based on the dark bands of myosin (A-bands) and the light bands of actin (I-bands). The pattern was used to identify myofibrils that were not damaged and to measure their initial sarcomere length (SL). The chosen myofibril or a small bundle of myofibrils was glued (3145 RTV MIL-A-46146 Adhesive; Dow Corning, Auburn, MI) and suspended between the tips of a rigid glass microneedle and a silicon atomic force cantilever (ATEC-CONTPt-20; Nanosensors, Watsonville, CA). The glue has a tensile strength of 1035 psi (7.14 MPa) and an estimated axial stiffness of 15,000 nN/μm. In contrast, the tensile forces in our experiments were ~45 kPa and the myofibril stiffness is <1800 nN/μm (see in Results). Therefore, the compliance of the glue should not have any influence in our experiments.

The microneedle stretched and shortened the myofibril using a piezoelectric controller. A laser system tracked the cantilever as it deflected due to changes in length of the myofibril. The microneedle motion, cantilever deflection, and cantilever stiffness were used to calculate the sarcomere length, force of the myofibrils, and sarcomere stiffness.

Stiffness of the cantilever

The cantilever stiffness was determined by measuring its dimensions through scanning electron microscope (Fig. 1) images (24,25) using

$$k_C = \frac{3EI}{L^3}, \tag{1}$$

where E is the Young's modulus (169 GPa for the silicon cantilevers (24)), I is the moment of inertia of the cross section of the cantilever, and L is the length of the cantilever from the base of the cantilever until the point of force action (25). The moment of inertia of a rectangular cross section is given by

$$I = \frac{W\ T^3}{12}, \tag{2}$$

where W is the width of the cantilever, and T is its thickness of the cantilever.

The cantilever has a rectangular profile at its base with length L_2, and a triangular profile at its tip with length L_1 (Fig. 2). Both the profiles have the same rectangular cross section with different widths, but the same thickness, T. The change in width is approximated by the average cantilever width, $\overline{W}$. Accordingly, the moment of inertia is approximated using

$$I = \frac{\overline{W}\ T^3}{12}. \tag{3}$$

The average width, $\overline{W}$, is given by

$$\overline{W} = \frac{L_2}{L}W + \frac{L_1}{L}\frac{W}{2}. \tag{4}$$

The $W/2$ term approximates the average width during the triangular part of the cantilever profile. The $L_2/2$ and $L_1/2$ terms represent the ratio of the length from the rectangular profile and the triangular profile, respectively. For simplicity, the cantilever stiffness can be rewritten as

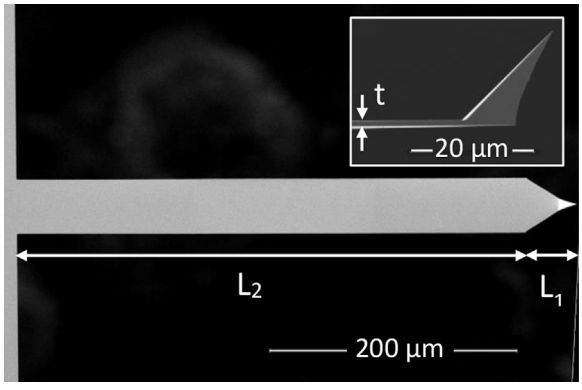

FIGURE 1 Scanning electron microscope image of the top view of the cantilever. The cantilever profile changes from rectangular to triangular at the tip of the cantilever. The inset shows a side view of the cantilever thickness and the cantilever tip where a myofibril is glued.

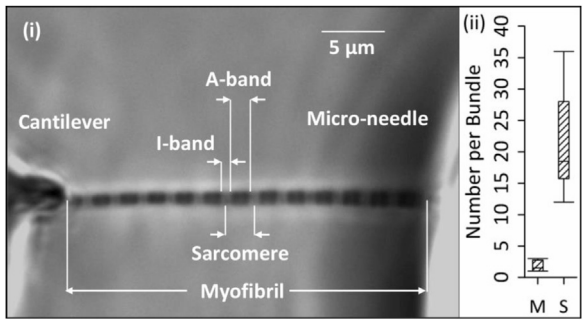

FIGURE 2 (*i*) Example of a psoas myofibril suspended between a cantilever and microneedle in rigor solution with a resting SL of 2.38 μm. (*ii*) Box-and-whisker plots summarize the number of myofibrils (*M*) and sarcomeres (*S*) within all the tested myofibril samples.

$$k_C = \frac{3E}{L^3}\left[\frac{1}{12}\left(\frac{L_2}{L}W + \frac{L_1}{L}\frac{W}{2}\right)T^3\right]. \quad (5)$$

The cantilevers used in these experiments had a stiffness of 40.27 nN/μm.

Force, sarcomere length, and stiffness calculations

The force of a single myofibril is equivalent to the force of a single sarcomere because sarcomeres are connected in series in a myofibril. The force is calculated using

$$F(t) = \frac{k_C\, c(t)}{M_N}, \quad (6)$$

where $F(t)$ is the force per myofibril as a function of time (t), M_N is the number of myofibrils in a tested bundle, $c(t)$ is the tip displacement of the cantilever (sampling rate: 0.2 MHz averaged over 1280 data points), and k_C is the cantilever stiffness as defined in Eq. 5.

The sarcomere length was calculated using

$$S(t) = \frac{M(0) - [c(t) - c(0)] + [n(t) - n(0)]}{S_N}, \quad (7)$$

where $S(t)$ represents the average sarcomere length as a function of time and captures the central tendency of the sarcomeres, given any nonuniformity of the different sarcomeres within a myofibril. Hence, "sarcomere length" refers to the average sarcomere length of the different sarcomeres in the myofibril. Moreover, $M(0)$ is the myofibril length at rest, $c(0)$ is the initial position of the cantilever tip, $n(t)$ is the input motion of the microneedle, $n(0)$ is the initial position of the microneedle, and S_N is the number of sarcomeres within the myofibril.

Four interventions were used to minimize the random errors in $F(t)$ and $S(t)$. First, cantilever displacement was calibrated to the laser-tracking system before the start of each experimental set. Second, the microneedle did not deflect during the experiments because it was made at least 20 times thicker than the cantilever. Third, the piezoelectric controller used to control the microneedle had a resolution greater than the noise of the system and did not limit the detectability of the myofibril response. Fourth, myofibrils with large numbers of sarcomeres were chosen to make sure that the sarcomere length represents the average length of the sarcomeres, not considering any nonuniformity in behavior.

To compare our results to other studies, the force, sarcomere length, and stiffness were normalized per cross-sectional area and the values were converted to half-sarcomere lengths. The average circular cross-section area of individual myofibrils was 1.77 μm^2, and the average diameter was 1.5 μm.

TABLE 1 Summary of the Microneedle Input Conditions for the Main Stretch and Main Shortening

Microneedle Input Condition	Displacement per Sarcomere (μm)	Speed (μm/s)
1	0.1	0.4
2	0.1	0.8
3	0.2	0.4
4	0.2	0.8
5	0.3	0.4
6	0.3	0.8
7	0.1	0.4

Repeatability was verified by repeating the first test at the end of an experimental set (conditions 1 and 7).

Experimental protocol

The myofibrils were placed in rigor solution and held taut at a resting position with no tensile force. The myofibrils were then stretched two consecutive times and then shortened two consecutive times. The first stretch and last shortening are referred to as the "prestretch" and "postshortening", respectively. The prestretch added some tension to the myofibril and removed any remaining slack. The postshortening brought the myofibril back to its initial position. Both movements were similar in every experiment with a total absolute displacement of 0.1 μm/sarcomere and a nominal speed of 0.4 μm/s. The second stretch and third shortening are referred to as the "main stretch" and the "main shortening", respectively. The displacement and speed for the main stretch and main shortening was maintained at seven different conditions in a series of experiments on the same myofibril (summarized in Table 1). The sarcomere stiffness was calculated by measuring the change in force and sarcomere length from the main stretch and the main shortening. Note that all the movements in the experiment were followed by a period of no activity to allow the myofibril to stabilize at a new length. It is important to note that the changes in sarcomere length can be lower than the length change imposed to the myofibrils due to compliance of the system. Most importantly, the actual velocity imposed during length changes is lower than the velocity dictated by the microneedle input. In our case, the actual velocities are between ~0.015- and ~0.03-μm/sarcomere/s.

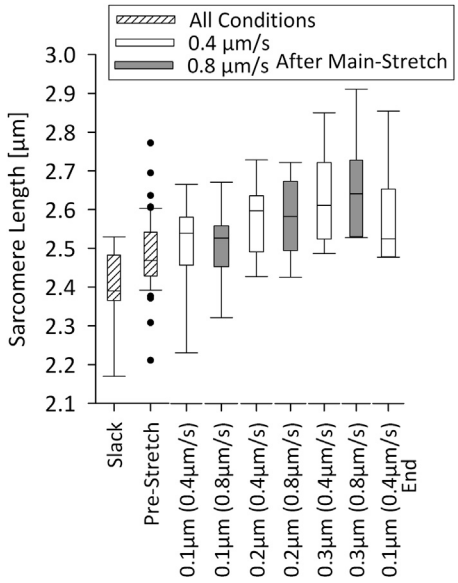

FIGURE 3 Box-and-whisker plots summarizing the resting SL, SL after the prestretch, and the SLs after the main stretch. Note that eight psoas myofibril samples were used in nine experimental sets.

Statistical analysis

The main stretch and main shortening from each condition were grouped and compared using a one-way analysis of variance (ANOVA) for repeated measures and coupled with a post hoc analysis using a Holm-Sidak test. In the cases where data did not follow a normal distribution, a one-way ANOVA for repeated measures on rank was performed and coupled with a post hoc analysis using a Turkey test. To evaluate if microneedle displacement and speed affected the main stretch and main shortening, a two-way repeated measures ANOVA was performed and coupled with a post hoc analysis using a Holm-Sidak test. A significance value of 5% ($p < 0.05$) was adopted in all comparisons. Box plots were used to summarize some data sets with the median ± interquartile range (box), the ± range (whiskers), and the outliers (points > 1.5 the box length).

RESULTS

Tested conditions

Repeated experiments were conducted on eight myofibril samples. Fig. 2 shows an example and summary of the initial characteristics for all the tested myofibrils. Multiple light microscopy images were used to determine the initial characteristics and each of these images focused on different parts of the myofibrils. Fig. 3 summarizes the resting SL, the SL after the prestretch, and the SLs after the main stretch. Notably, the SLs are within the physiological range for skeletal myofibrils. Furthermore, the main stretch ended roughly at the SL at which the main shortening started.

Force and sarcomere lengths

Representative force and sarcomere length records show the first six tested conditions (Fig. 4). Using condition 1 as an example (Fig. 4 (*i*)), the myofibrils were first set to a resting SL (annotated by (*a*) in the SL plots: 2.53 μm). The myofibrils were then stretched to a new SL (prestretched, *b*, 2.60 μm) and stabilized (*c*, 2.61 μm). Next, the myofibrils were stretched again and the SL increased (main stretch, *d*, 2.66 μm). After the myofibril stabilized, the force slightly dropped and the SL slightly increased (*e*, 2.67 μm). The myofibril was then shortened and the SL dropped (main shortening, *f*, 2.62 μm). Finally, the

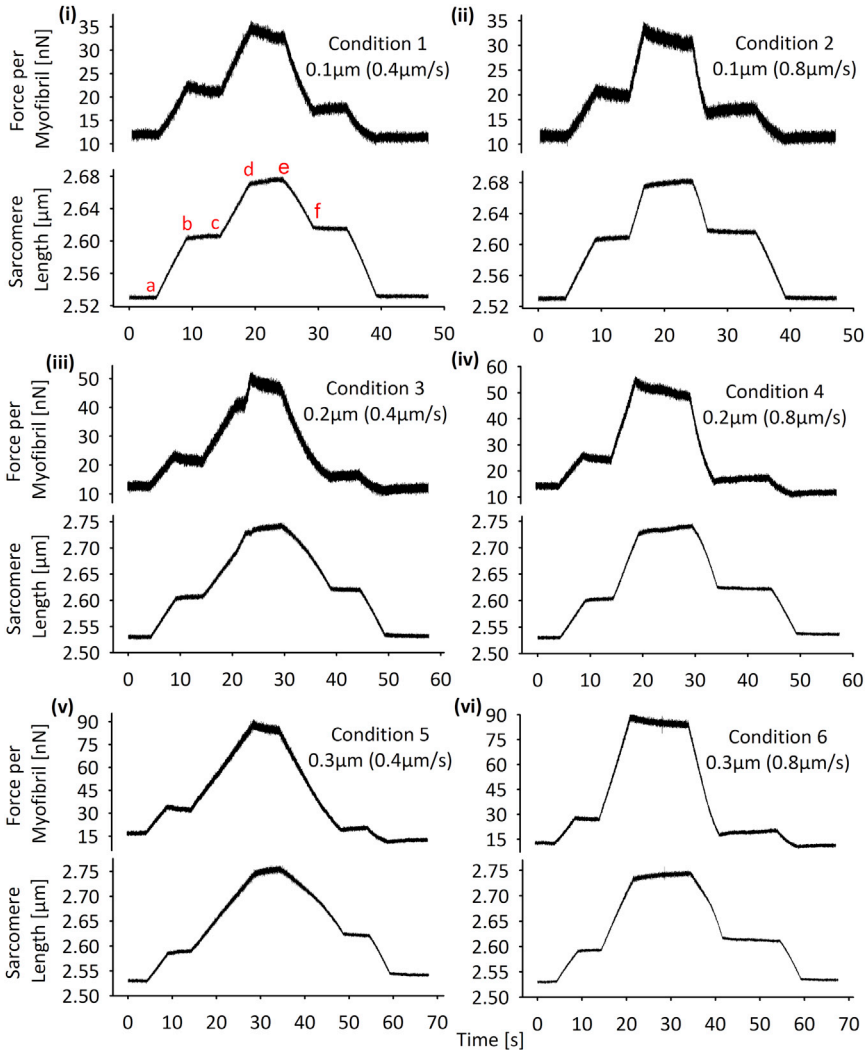

FIGURE 4 Representative plots (*i–vi*) of the force per myofibril and SL as a function of time for experiments on the same myofibril. The SL plot in (*i*) is annotated with letters (*a*) to (*f*) to show the experimental steps. To see this figure in color, go online.

myofibril was shortened back to the initial position (post shortening, *a*, 2.53 μm). In this example, the main shortening (*e* to *f*) showed a sarcomere stiffness of 282 nN/μm as compared to 189 nN/μm during the main stretch (*c* to *d*). The discrepancy resulted from the main shortening having 28.3% more change in force and 13.9% less change in SL, which is equivalent to 49.0% higher sarcomere stiffness. Similar trends were seen for the rest of the conditions (Fig. 4 (*ii–vi*)).

Compliances in the attachments of the myofibrils to the cantilever and the microneedle may affect the results that we observed, especially when calculating the sarcomere length changes (Eq. 7). Accordingly, we have performed some experiments ($n = 3$) in which we attached the myofibrils to the cantilever and microneedle without using glue (just by adherence). The results are consistent with the experiments that have used glue, confirming that the interpretation of the data is not affected by the mode of attachments of the myofibrils (Supporting Material).

The change in force, change in SL, and sarcomere stiffness were compared for the main stretch and the main shortening for all the tested myofibrils (Fig. 5). The main shortening was different when compared to the main stretch.

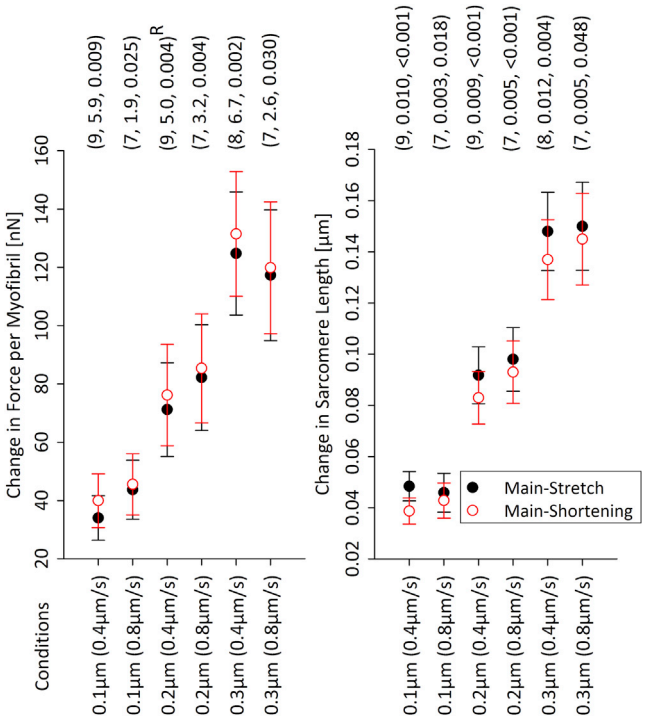

FIGURE 5 Mean ± SE of the absolute value for the change in force per myofibril and change in sarcomere length of the main stretch and main shortening. Three parenthesized values are shown above each group—sequentially: number of observations, difference in mean values (a symbol (—) is used when no statistically significant difference is present), and *p* value arising from the one-way ANOVA for repeated measures. Some parentheses have an *R* symbol to indicate the use of a one-way ANOVA for repeated measures on ranks. To see this figure in color, go online.

It showed a larger change in force per myofibril and larger sarcomere stiffness, but smaller change in SL. To confirm that the velocities that we used in our experiments would be comparable to experiments using higher velocities of length changes, we performed additional experiments ($n = 3$) in which we used a considerably higher velocity (1000 μm/s). The results follow a similar trend to the experiments at lower velocities throughout this study (Fig. S1).

To estimate the stiffness, we plotted the relation between force and sarcomere length changes during the main stretch and main shortening (Fig. 6). As expected, there is a hysteresis in the force during the stretch-shortening cycles for all conditions.

Using these plots, we estimated the linear stiffness to determine the effect of speed and displacement on the main stretch and main shortening (Fig. 7). We linearly estimated the stiffness using the change in force per myofibril and change in SL at the start and the end of the mechanical perturbations. The results show that the stiffness was different during stretch and shortening. Similar results were observed if no glue was used for myofibril attachment (Figs. S2 and S3).

Experimental repeatability

Although it is challenging to certify that the myofibrils are intact throughout our experiments, we tested the reliability of our results by repeating the first experiment (condition 1, 0.1 μm (0.4 μm/s)) at the end of each experimental set (condition 7, 0.1 μm (0.4 μm/s) − End). Fig. 8 shows a typical example from both these experiments on the same myofibril.

The change in force per myofibril, change in SL, and sarcomere stiffness were compared for the start and end experiments for all the tested myofibrils (Fig. 9). When comparing the main stretch and the main shortening, the start and end experiments showed that the results were repeatable and that the protocol used in the experiments did not affect the main results and conclusions of this article.

DISCUSSION

We observed that the myofibrils isolated from psoas muscles presented a stiffness-under-rigor condition that was independent of speed and displacement during stretch (987 nN/μm.sarcomere). During shortening, the sarcomere stiffness was independent of displacement, but dependent on speed (1234 nN/μm.sarcomere at 0.4 μm/s; 1106 nN/μm.sarcomere at 0.8 μm/s). Furthermore, the myofibril stiffness during shortening was greater than that during stretching (31% at 0.4 μm/s; 8% at 0.8 μm/s). Overall, these results suggest that the measured sarcomere stiffness is nonlinear, and a function of the direction and speed, but not the magnitude of the length changes. It may be noted that our results do not fit with ideas that the cross-bridge

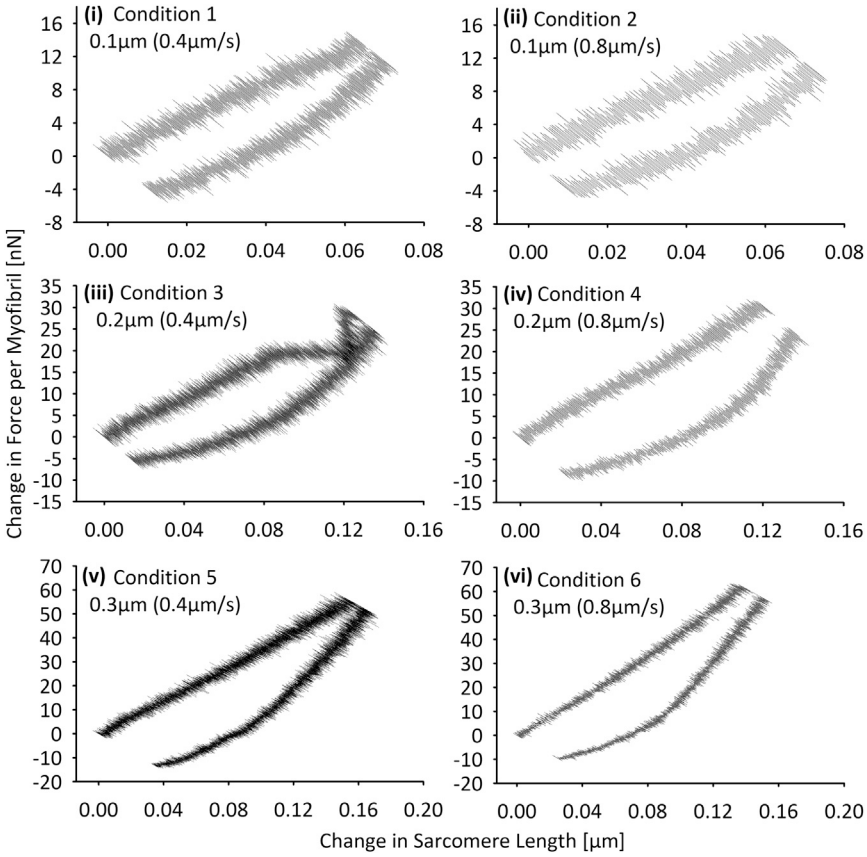

FIGURE 6 Representative plots (*i–vi*) of the change in force per myofibril as a function of the change in sarcomere length during the main stretch (*c* to *d*) and main shortening (*e* to *f*) stages. All the experiments in these plots used the same myofibril.

elasticity is nonlinear with lower stiffness at low (particularly negative) strain, as suggested by single molecule results by Kaya and Higuchi in 2010 (5). Such nonlinearity would, a priori, be expected to cause lower stiffness during the release than during the stretch (see Introduction), something that was not observed. However, because the cross-bridge compliance accounts for quite a low fraction of the total myofibril compliance in our experiments, it is possible that a small nonlinearity of the cross-bridge compliance is hidden by other effects.

Overall, it is difficult to compare our results with other studies, as other laboratories did not measure sarcomere stiffness using single myofibrils. Furthermore, the studies that used single fibers have used different conditions (i.e., stretch magnitude, speed, preparations). A study by Suzuki and Sugi (9) used rabbit psoas fibers in rigor and measured sarcomere stiffness with 10–30% stretches (change in SL: 0.28–0.43 μm; range of SLs: 2.58–2.88 μm; speed of stretch: $<$1000 μm/s). The authors observed an extension of myosin in the bare region of the H-zone (myosin stiffness of $\sim 3.6 \times 10^4$ pN per unit length). Moreover, the 10–20% stretches repeatedly extended actin outside the overlap region of the I-band (actin stiffness of $\sim 2.4 \times 10^4$ pN per unit length). This is the only study that stretched fibers in rigor with a similar range used in this article, but with faster speed. The stiffness reported in their study is within the magnitude observed in our experiments ($\sim 8.4 \times 10^4$ pN per unit length) and agreed with previous findings (1.8×10^4 pN per unit length) (26).

Other studies on fibers in rigor used stretches below the resting SL and with a markedly smaller change in the half-sarcomere length (hs): 0.5–8 nm (6,10–12,27). Linari et al. (6,27) studied frog tibialis anterior fibers and rabbit psoas fibers that were stretched by 3–5 nm/hs and showed a half-sarcomere compliance of 28.2 nm/MPa (stiffness, 35.3 kPa/nm). The attached myosin heads resulted in 26% of the compliance (compliance, 7.2 nm/MPa; stiffness, 138.9 kPa/nm; average stiffness per myosin head, 1.21 pN/nm). The remaining 74% resulted from the actin filaments (compliance, 21.0 nm/MPa; stiffness, 47.6 kPa/nm). A study by Higuchi et al. (11) stretched rabbit psoas fibers by 0.5–2 nm/hs and suggested that 55% of the total sarcomere compliance resulted from actin in the I-band region. At an SL of 1.8 μm, the compliance was 12 PM/hs per 1 kN/m^2 (stiffness, 83.3 kPa/nm.hs). At an SL of 2.4 μm, the compliance was 25 PM/hs per 1 kN/m^2 (stiffness, 40 kPa/nm.hs). Furthermore, the actin filament compliance was greater at lower fiber tension. Accordingly, it was concluded that sarcomere compliance is associated with either nonlinear elasticity of actin or slack filaments at low tension. Fusi et al. (12) stretched frog fibers by 2–8 nm/hs and found that the stiffness was linear for the

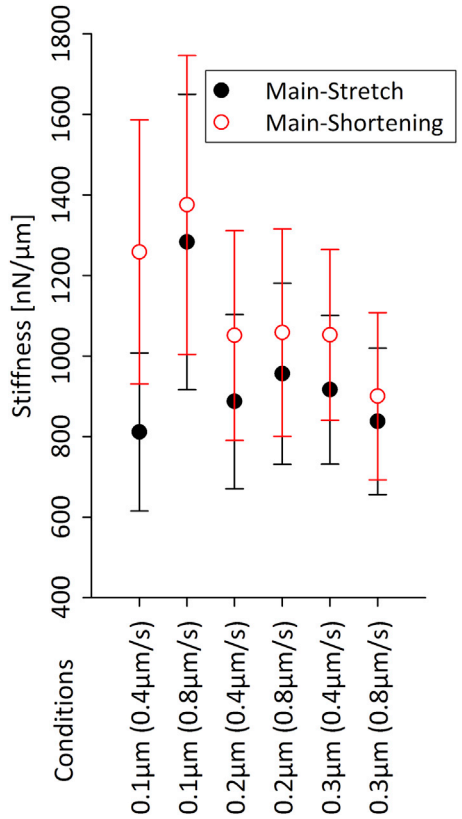

FIGURE 7 Stiffness during the main stretch and main shortening for the different experimental conditions. Plots summarize the effect of the microneedle input speed and displacement on the main stretch and main shortening. To see this figure in color, go online.

sarcomeres, myosin and actin filaments, and the cross-bridges. Independent of the initial fiber tension (up to 275 kPa), the half-sarcomere stiffness ranged from 0.415 to 0.424 T_0/nm (equivalent to 58.9–60.2 kPa/nm.hs; T_0 = 142 kPa). Yamamoto and Herzig (10) stretched frog fibers by 3–6 nm/hs and found that the stiffness was 2215 N/cm.hs per fiber.

To summarize the previous paragraph, studies of muscle fibers in rigor with appreciably smaller stretches (6,11,12,27) than used in this study report stiffness values that are an order-of-magnitude greater than the values we observed (~1 kPa/nm). The smaller stretches also resulted in stiffness values that may be attributed to the actin filaments and the cross-bridges. Nevertheless, if stiffness had been an order-of-magnitude greater than what we measured, then the myofibrils in this article would either show forces in the order of 2000 kPa or displacements of ~1 nm/hs. These force and displacement values are significantly outside the ranges that we observed and cannot be attributed to experimental error. The most likely explanation for the discrepancy between the present and previous results is the presence of elements within the myofibril preparation that act in series with the sarcomeres (myofibrils + cross-bridges) during imposed length changes. Such series elastic elements may result from sarcomere nonuniformities with weak sarcomeres particularly at the myofibril ends. In a separate analysis of three myofibrils for which we succeeded in obtaining high-quality microscope images, we found that the sarcomere length change during an imposed length change was appreciably larger at the myofibril ends than in the center. This simple analysis suggests that the measured stiffness is determined by different sarcomere components: 1) cross-bridges and myofilaments in the strongest sarcomeres where the sarcomere length change is minimal, 2) titin elasticity in the weakest sarcomeres that elongate most, and 3) combinations of these factors and shearing effects in other sarcomeres. Our data are too complex to provide conclusive insights about the characteristics of the cross-bridge elasticity, i.e., whether it is linear or nonlinear. An interesting element of our results is the exceptional stability of the myofibril preparations over the course of the demanding experiments even though they have visible nonuniformities and are not supported by a cytoskeletal scaffold as in muscle cells. This suggests that the myofibril internally holds a system that protects it against severe irreparable mechanical damage.

Based on our findings and the literature data, we suggest that sarcomeres in rigor have viscoelastic properties. Thus, sarcomere stiffness is different during stretching and shortening, and the difference depends on the speed of the length changes.

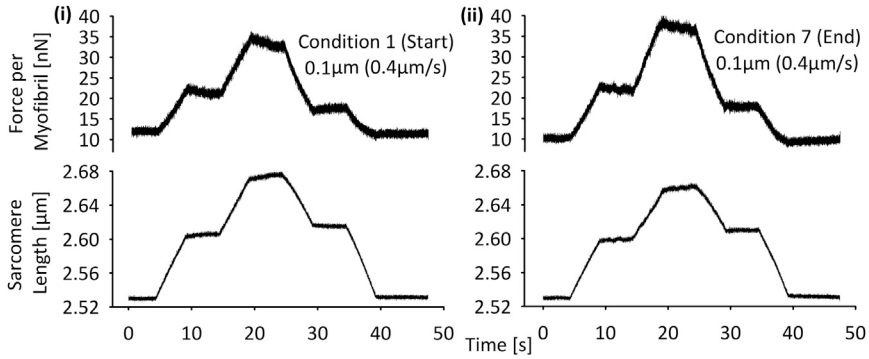

FIGURE 8 Representative plots (*i* and *ii*) showing the start and end tests of a given experimental set with the same myofibril. Both cases used the same condition (0.1 μm (0.4 μm/s)).

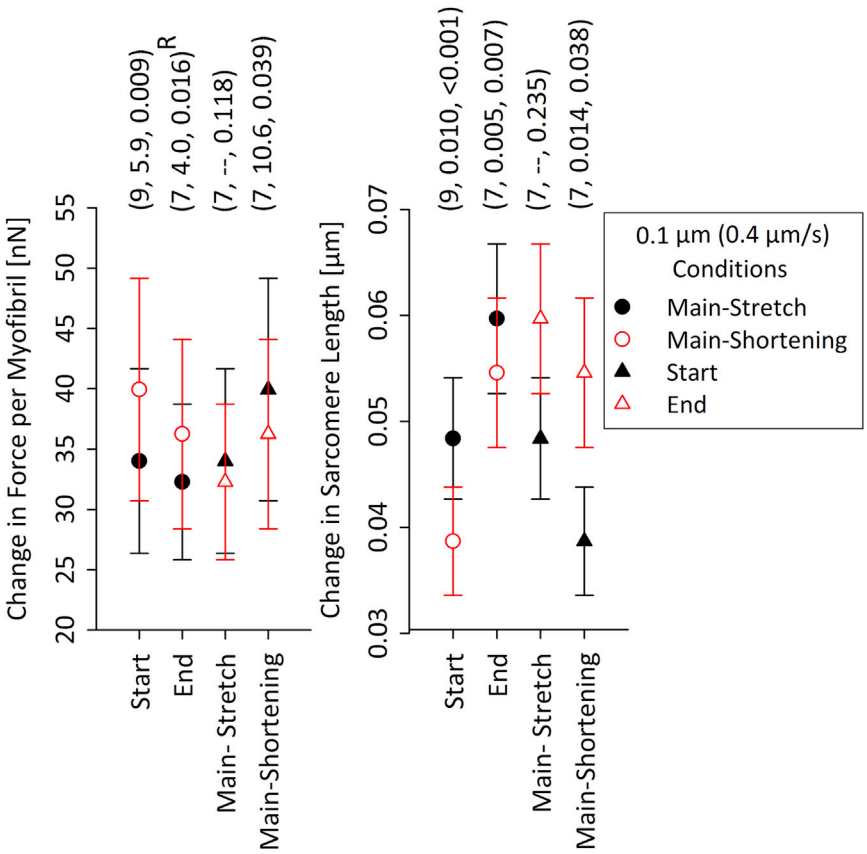

FIGURE 9 Mean ± SE of the absolute value for the change in force per myofibril and change in sarcomere length for the 0.1 μm (0.4 μm/s) condition at the start and the end of each experimental set. The main stretch from the start experiments is compared to the main stretch and the main shortening from the end experiments. Similarly, the main shortening from the start experiment is compared to the main stretch and the main shortening from the end experiments. Three parenthesized values are shown above each group—sequentially: number of observations, difference in mean values (a symbol (—) is used when no statistically significant difference is present), and p value arising from the one-way ANOVA for repeated measures. Some parentheses have an R symbol to indicate the use of a one-way ANOVA for repeated measures on ranks. To see this figure in color, go online.

SUPPORTING MATERIAL

Three figures are available at http://www.biophysj.org/biophysj/supplemental/S0006-3495(17)31118-9.

AUTHOR CONTRIBUTIONS

N.S. assembled, improved, and validated the custom-AFM, helped design the study and draft the manuscript, and performed the experiments and data analyses. M.P. performed some of the experiments and helped design and draft the manuscript. A.M. helped design the study and draft the manuscript. S.V. co-supervised the study and helped draft the manuscript. D.E.R. co-supervised the study and helped design the study and draft the manuscript. All authors gave approval for publication, agreed to be accountable for all aspects of the work, have no competing interests, and are qualified for authorship.

ACKNOWLEDGMENTS

The authors thank Albert Kalganov for providing the scanning electron microscope images used to calibrate the cantilevers. The research was performed at the Muscle Physiology and Biophysics Laboratory of McGill University.

This study was funded by the Canadian Institutes of Health Research, the Natural Sciences and Engineering Research Council of Canada, and the Swedish Research Council. D.E.R. is a Canada Research Chair in Muscle Biophysics. A.M. was a visiting scholar at McGill University funded by the Wenner-Gren Foundation and by Linnaeus University, Faculty of Health and Life Sciences. A.M. was also funded by the Swedish Research Council (grant No. 2015-05290). M.P. was funded by Linnaeus University, Faculty of Health and Life Sciences, and the Swedish Research Council (grant No. 2015-00385).

REFERENCES

1. Huxley, A. F. 1957. Muscle structure and theories of contraction. *Prog. Biophys. Biophys. Chem.* 7:255–318.
2. Huxley, A. F., and R. M. Simmons. 1971. Proposed mechanism of force generation in striated muscle. *Nature.* 233:533–538.
3. Rassier, D. E. 2008. Pre-power stroke cross bridges contribute to force during stretch of skeletal muscle myofibrils. *Proc. Biol. Sci.* 275:2577–2586.
4. Ranatunga, K. W., H. Roots, G. J. Pinniger, and G. W. Offer. 2010. Crossbridge and non-crossbridge contributions to force in shortening and lengthening muscle. *Adv. Exp. Med. Biol.* 682:207–221.
5. Kaya, M., and H. Higuchi. 2010. Nonlinear elasticity and an 8-nm working stroke of single myosin molecules in myofilaments. *Science.* 329:686–689.
6. Linari, M., M. Caremani, …, V. Lombardi. 2007. Stiffness and fraction of myosin motors responsible for active force in permeabilized muscle fibers from rabbit psoas. *Biophys. J.* 92:2476–2490.
7. Cecchi, G., M. A. Bagni, …, P. J. Griffiths. 2003. Use of sinusoidal length oscillations to detect myosin conformation by time-resolved x-ray diffraction. *Adv. Exp. Med. Biol.* 538:267–277, discussion 277.
8. Kaya, M., and H. Higuchi. 2013. Stiffness, working stroke, and force of single-myosin molecules in skeletal muscle: elucidation of these

mechanical properties via nonlinear elasticity evaluation. *Cell. Mol. Life Sci.* 70:4275–4292.

9. Suzuki, S., and H. Sugi. 1983. Extensibility of the myofilaments in vertebrate skeletal muscle as revealed by stretching rigor muscle fibers. *J. Gen. Physiol.* 81:531–546.
10. Yamamoto, T., and J. W. Herzig. 1978. Series elastic properties of skinned muscle fibres in contraction and rigor. *Pflugers Arch.* 373:21–24.
11. Higuchi, H., T. Yanagida, and Y. E. Goldman. 1995. Compliance of thin filaments in skinned fibers of rabbit skeletal muscle. *Biophys. J.* 69:1000–1010.
12. Fusi, L., M. Reconditi, …, G. Piazzesi. 2010. The mechanism of the resistance to stretch of isometrically contracting single muscle fibres. *J. Physiol.* 588:495–510.
13. Lewalle, A., W. Steffen, …, J. Sleep. 2008. Single-molecule measurement of the stiffness of the rigor myosin head. *Biophys. J.* 94:2160–2169.
14. Kawai, M., and P. W. Brandt. 1980. Sinusoidal analysis: a high resolution method for correlating biochemical reactions with physiological processes in activated skeletal muscles of rabbit, frog and crayfish. *J. Muscle Res. Cell Motil.* 1:279–303.
15. Cooke, R., and K. Franks. 1980. All myosin heads form bonds with actin in rigor rabbit skeletal muscle. *Biochemistry.* 19:2265–2269.
16. Schoenberg, M., and E. Eisenberg. 1985. Muscle cross-bridge kinetics in rigor and in the presence of ATP analogues. *Biophys. J.* 48:863–871.
17. Månsson, A., D. Rassier, and G. Tsiavaliaris. 2015. Poorly understood aspects of striated muscle contraction. *BioMed Res. Int.* 2015:245154.
18. Fabiato, A. 1988. Computer programs for calculating total from specified free or free from specified total ionic concentrations in aqueous solutions containing multiple metals and ligands. *Methods Enzymol.* 157:378–417.
19. Rassier, D. E., W. Herzog, and G. H. Pollack. 2003. Dynamics of individual sarcomeres during and after stretch in activated single myofibrils. *Proc. Biol. Sci.* 270:1735–1740.
20. Minozzo, F. C., and D. E. Rassier. 2010. Effects of blebbistatin and Ca^{2+} concentration on force produced during stretch of skeletal muscle fibers. *Am. J. Physiol. Cell Physiol.* 299:C1127–C1135.
21. Cornachione, A. S., and D. E. Rassier. 2012. A non-cross-bridge, static tension is present in permeabilized skeletal muscle fibers after active force inhibition or actin extraction. *Am. J. Physiol. Cell Physiol.* 302:C566–C574.
22. Shalabi, N., A. Cornachione, …, D. E. Rassier. 2017. Residual force enhancement is regulated by titin in skeletal and cardiac myofibrils. *J. Physiol.* 595:2085–2098.
23. Labuda, A., T. Brastaviceanu, …, D. E. Rassier. 2011. Optical detection system for probing cantilever deflections parallel to a sample surface. *Rev. Sci. Instrum.* 82:013701.
24. Hopcroft, M. A., W. D. Nix, and T. W. Kenny. 2010. What is the Young's modulus of silicon? *J. Microelectromech. Syst.* 19:229–238.
25. Lübbe, J., L. Doering, and M. Reichling. 2012. Precise determination of force microscopy cantilever stiffness from dimensions and eigenfrequencies. *Meas. Sci. Technol.* 23:045401.
26. White, D. C. S., and J. Thorson. 1973. The kinetics of muscle contraction. *Prog. Biophys. Mol. Biol.* 27:173–255.
27. Linari, M., I. Dobbie, …, V. Lombardi. 1998. The stiffness of skeletal muscle in isometric contraction and rigor: the fraction of myosin heads bound to actin. *Biophys. J.* 74:2459–2473.